Stability and error analysis of a third order fully discrete local discontinuous Galerkin methods for high order wave equations

Haijin Wang[†] Qiang Zhang [‡] Chi-Wang Shu [§] Qi Tao [¶*]

Abstract

Due to the lack of coercivity and the fact that the corresponding local discontinuous Galerkin (LDG) operator is not symmetric, it is challenging to establish an energy analysis for implicit-explicit (IMEX) LDG schemes for high order wave equations, especially for high order schemes. As a first step towards resolving this problem, we study high order IMEX-LDG schemes for high order wave equations which only contain the highest spatial derivative term (hence the time discretization method becomes a purely implicit one). The unconditional energy stability analysis of the fully discrete schemes which couple a third order Runge-Kutta type IMEX method with LDG spatial discretization methods will be presented. The main technique is introducing a series of temporal differences about stage solutions and constructing a semi-negative definite symmetric form about the discretization for the highest order derivative terms. By the aid of a special projection operator and exploiting the stability provided by the temporal differences, we also obtain optimal error estimates for the fully discrete schemes. Numerical experiments for both the third order and the fifth order wave equations are displayed, which show the optimal accuracy of the considered schemes as well as the good performance of the schemes in simulating solitary waves.

Keywords. local discontinuous Galerkin, implicit-explicit, wave equations, stability, error estimates.

AMS classification. 65M12, 65M60

1 Introduction

High order wave equations arise from many physical applications. For example, the famous Korteweg-de Vries (KdV) type equations [4] describe the propagation of dispersive waves in aerology, geology, oceanography, plasma physics and other fields, the fifth order wave

*Corresponding author.

[†]College of Science, Nanjing University of Posts and Telecommunications, Nanjing 210023, Jiangsu Province, P. R. China. E-mail: hjwang@njupt.edu.cn. Research partially supported by NSFC grant 12071214.

[‡]Department of Mathematics, Nanjing University, Nanjing 210093, Jiangsu Province, P. R. China. E-mail: qzh@nju.edu.cn. Research partially supported by NSFC grant 12071214.

[§]Division of Applied Mathematics, Brown University, Providence, Rhode Island 02912. E-mail: chi-wang_shu@brown.edu. Research partially supported by NSF grant DMS-2309249.

[¶]School of Mathematics, Statistics and Mechanics, Beijing University of Technology, Beijing 100124, P. R. China. E-mail: taoqi@bjut.edu.cn. Research partially supported by NSFC grant 12301464.

equations simulate the surface-tension model such as the long waves in shallow liquid under ice cover [21]. Among the various numerical methods for solving such equations, local discontinuous Galerkin (LDG) method [9] is one of the efficient methods. It was proposed by Cockburn and Shu in [9] for solving convection-diffusion equations, and later it was developed for solving many types of partial differential equations (PDEs) containing high order spatial derivatives, see for example [37, 19, 30, 31, 32, 15, 33, 34, 40, 38] as an incomplete list of references. The LDG method has several advantages such as its flexibility for *hp*-adaptivity and its local solvability, namely, the auxiliary variables approximating the derivatives of the solution can be locally eliminated.

Even though there is plenty of work on the LDG methods for high order wave equations, the theoretical analysis for the fully discrete LDG schemes is relatively rare. We would like to consider the stability and error analysis of fully discrete LDG schemes for the following third order and fifth order wave equations

$$U_t + f(U)_x = U_{xxx}, \tag{1.1}$$

$$U_t + f(U)_x = U_{xxxxx}, \tag{1.2}$$

where $x \in \Omega = (x_l, x_r)$ and $t \in (0, T]$, $f(U)$ is the convection flux. The initial condition is

$$U(x, 0) = U_0(x), \qquad x \in \Omega, \tag{1.3}$$

where $U_0(x) \in L^2(\Omega)$. We only consider periodic boundary condition for simplicity.

For the above high order wave equations, explicit time discretization methods require very small time step to ensure the stability of the ODE system which is derived from the LDG spatial discretization, while fully implicit time discretization methods require solving nonlinear systems. So an efficient time discretization technique could be semi-implicit, treating the linear (or stiff) part implicitly and the nonlinear (or nonstiff) part explicitly, such as the spectral deferred correction (SDC) method [16, 28], the exponential time differencing (ETD) method [11] and the implicit-explicit (IMEX) method [2, 1].

The Runge-Kutta type IMEX (IMEX-RK) time discretization methods coupled with LDG spatial discretization have been investigated for convection-diffusion equations and time dependent fourth order PDEs [25, 27], where the time steps are allowed to be independent of the mesh size. Such type of time discretization methods are also efficient for high order wave equations, see for example the numerical experiments in [28, 17, 40, 20, 38] and the formal Fourier analysis in [23], while there is rare theoretical analysis of the fully discrete IMEX-LDG schemes for solving high order wave equations. Recently, the authors of the present work gave a first attempt on energy analysis of IMEX-LDG schemes for the linearized KdV equations in [26], but only first and second order IMEX-RK schemes were considered in time discretization.

For higher order IMEX-RK schemes, the corresponding energy analysis becomes more challenging due to the intricate relationships between intermediate stages as well as the complex interaction between the explicit and implicit discretizations. To overcome these difficulties, first we need to explore the stability mechanism of the purely explicit and the purely implicit parts. With regard to the explicit part, one can follow the framework established in [35] for explicit Runge-Kutta discontinuous Galerkin (RKDG) methods, by using the temporal difference technique. For the implicit part, a related work by Sun et al.

[22] established energy inequalities for all diagonal Padé approximations by an analytical Cholesky type decomposition of symmetric matrices. Note that the technique of [22] is suitable for purely implicit schemes, but is not easy to extend to IMEX schemes. Moreover, since the temporal difference technique was successfully applied to derive the stability of lower order in time IMEX-LDG methods for KdV equations in [26], we think it will be helpful for the high order in time IMEX-LDG methods. But we have to admit that, at present we are not able to solve the interaction between the explicit and implicit discretizations for high order in time IMEX-LDG methods, due to some technical difficulties. So the stability of high order IMEX-LDG methods for the wave equation (1.1) and (1.2) with the convection term $f(U) \neq 0$ is not available at present.

As a first step towards establishing the energy analysis for the high order IMEX-LDG scheme for high order wave equations, the main objective of this paper is to study the unconditional stability and optimal error analysis of the fully discrete LDG scheme coupled with a third order IMEX-RK time discretization method [1], for solving equations (1.1) and (1.2) with the convection flux $f(U) = 0$. Even in this case, the analysis is non-trivial, the main difficulty lies in the construction of suitable energy equations. Since the LDG operators for the dispersive equations are not symmetric and they lack coercivity, the energy analysis for the implicit part is totally different from that for the dissipative equations [25, 27, 5].

In this paper, we will adopt the temporal difference technique mentioned above to carry out the energy analysis. In detail, we first introduce a suitable series of temporal differences about stage solutions, then the energy stability analysis starts from the energy equation $\|u^{n+1}\|^2 - \|u^n\|^2 = \mathcal{RHS}(u^n)$, where $\mathcal{RHS}(u^n)$ is made up of the inner products of the temporal differences. To obtain the desired results, we have to carefully split the term $\mathcal{RHS}(u^n)$ into two parts, the first part reflects the stability mechanism from the temporal differences, and the second part needs to be converted to information of spatial discretization, which represents the stability of the spatial discretization for the third/fifth order derivative terms. During this process, we hope to construct a semi-negative definite symmetric form for the second part, meanwhile we hope the first part is no more than 0. Hence, the splitting is not trivial. We will introduce 13 undetermined parameters and solve a linear system with 10 equations to achieve our goal. Even though the same idea has been adopted in [26] for lower order schemes, here the analysis is much more involved, both the definition of temporal differences and the splitting process are much more complex. Furthermore, since the temporal difference is defined by the explicit part of the IMEX-RK scheme (see Remark 3.3), our analysis would be helpful for studying the stability of the corresponding schemes for (1.1) and (1.2) with the convection flux $f(U) \neq 0$, which is our long-term goal.

Regarding the error estimates, we would like to comment that it is difficult to obtain optimal error estimates by using the commonly-used Gauss-Radau (GR) projection [8], since the GR projection can not eliminate the interactive influences of errors at different intermediate stages, which prevents us from getting optimal error estimates. Thus, we adopt the projection technique proposed in [26], by which all the projection terms vanish in the error equations with respect to the auxiliary variables. By the aid of the new projection technique and by exploiting the stability provided by the temporal differences to control the projection related terms, we achieve optimal error estimates for the considered schemes. Several numerical experiments for both the third order and the fifth order wave equations

show the optimal accuracy of the considered schemes as well as the good performance of the schemes in simulating solitary waves.

The paper is organized as follows. In section 2 we present the semi-discrete LDG schemes for the wave equations (1.1) and (1.2) and some related properties, a brief introduction of the IMEX-RK schemes and third order in time fully discrete IMEX-LDG schemes for both (1.1) and (1.2) are also given in this section. In section 3 and section 4, we give the unconditional stability analysis and optimal error estimates for the fully discrete schemes with the convection flux $f(\cdot) = 0$, respectively. In section 5 we show some numerical results to verify the accuracy and the performance of the considered schemes. The conclusion is given in section 6.

2 Semi-discrete and fully discrete LDG schemes

In this section, we first introduce the semi-discrete LDG schemes for solving equations (1.1) and (1.2) and some properties of the semi-discrete LDG schemes, then we introduce the IMEX-RK time marching schemes and the corresponding fully discrete schemes.

2.1 The semi-discrete LDG schemes

Before presenting the semi-discrete LDG scheme, we give the partition of the computational domain $\Omega = (x_l, x_r)$, denoted by $\mathcal{T}_h = \{I_j = (x_{j-\frac{1}{2}}, x_{j+\frac{1}{2}})\}_{j=1}^{N}$, where $x_{\frac{1}{2}} = x_l$ and $x_{N+\frac{1}{2}} = x_r$. Let $h_j = x_{j+\frac{1}{2}} - x_{j-\frac{1}{2}}$ be the length of element I_j, for $j = 1, \ldots, N$, and we define the mesh size as $h = \max_j h_j$. In this paper, the partition $\mathcal{T}_h$ is assumed to be quasi-uniform, which means that there exists a positive constant ρ, such that $h_j/h \geq \rho$ for all j.

Associated with the above mesh $\mathcal{T}_h$, we define the discontinuous finite element space

$$V_h = V_h^k = \left\{ v \in L^2(\Omega) : v|_{I_j} \in \mathcal{P}_k(I_j),\ \forall j = 1, \ldots, N \right\}, \tag{2.1}$$

where $\mathcal{P}_k(I_j)$ represents the polynomial space in I_j with order of degree no more than k. As the practice in DG methods, we denote $v^+_{j+\frac{1}{2}}$ and $v^-_{j+\frac{1}{2}}$ as the trace values taken from the right and the left sides of the boundary point $x_{j+\frac{1}{2}}$, respectively, and the "jump" is represented as $[\![v]\!]_{j+\frac{1}{2}} = v^+_{j+\frac{1}{2}} - v^-_{j+\frac{1}{2}}$.

2.1.1 The semi-discrete LDG scheme for the wave equation (1.1)

Introducing two auxiliary variables $Q = U_x$ and $P = Q_x$, we can rewrite (1.1) into the following equivalent first order system

$$U_t + f(U)_x - P_x = 0, \tag{2.2a}$$
$$P - Q_x = 0, \tag{2.2b}$$
$$Q - U_x = 0. \tag{2.2c}$$

Then we define the semi-discrete LDG scheme for (1.1) as follows: find the map

$$\big(u(\cdot,t), p(\cdot,t), q(\cdot,t)\big) : [0,T] \to [V_h]^3,$$

such that the following variational forms

$$\begin{aligned}(u_t, v)_j - (f(u), v_x)_j + \hat{f}(u)_{j+\frac{1}{2}} v^-_{j+\frac{1}{2}} - \hat{f}(u)_{j-\frac{1}{2}} v^+_{j-\frac{1}{2}} \\ +(p, v_x)_j - \hat{p}_{j+\frac{1}{2}} v^-_{j+\frac{1}{2}} + \hat{p}_{j-\frac{1}{2}} v^+_{j-\frac{1}{2}} = 0, \end{aligned} \tag{2.3a}$$

$$(p, \phi)_j + (q, \phi_x)_j - \hat{q}_{j+\frac{1}{2}} \phi^-_{j+\frac{1}{2}} + \hat{q}_{j-\frac{1}{2}} \phi^+_{j-\frac{1}{2}} = 0, \tag{2.3b}$$

$$(q, \psi)_j + (u, \psi_x)_j - \hat{u}_{j+\frac{1}{2}} \psi^-_{j+\frac{1}{2}} + \hat{u}_{j-\frac{1}{2}} \psi^+_{j-\frac{1}{2}} = 0, \tag{2.3c}$$

hold in each cell I_j, for any test functions $v, \phi, \psi \in V_h$, where $(w, v)_j = \int_{I_j} w(x)v(x)dx$, $\hat{f}(u)$ is the numerical flux for the convection term and it is locally Lipschitz continuous and consistent with the flux f, the other hat terms $\hat{p}, \hat{q}, \hat{u}$ are numerical fluxes for the dispersion term and

$$\hat{p} = p^+, \quad \hat{q} = q^-, \quad \hat{u} = u^-. \tag{2.4}$$

With the notations

$$\mathcal{H}^c_j(f(u), v) = (f(u), v_x)_j - \hat{f}(u)_{j+\frac{1}{2}} v^-_{j+\frac{1}{2}} + \hat{f}(u)_{j-\frac{1}{2}} v^+_{j-\frac{1}{2}}, \tag{2.5}$$

$$\mathcal{L}^{\pm}_j(w, v) = (w, v_x)_j - w^{\pm}_{j+\frac{1}{2}} v^-_{j+\frac{1}{2}} + w^{\pm}_{j-\frac{1}{2}} v^+_{j-\frac{1}{2}}, \tag{2.6}$$

we can rewrite the above semi-discrete LDG scheme as

$$(u_t, v)_j = \mathcal{H}^c_j(f(u), v) - \mathcal{L}^+_j(p, v), \tag{2.7a}$$

$$(p, \phi)_j = -\mathcal{L}^-_j(q, \phi), \tag{2.7b}$$

$$(q, \psi)_j = -\mathcal{L}^-_j(u, \psi). \tag{2.7c}$$

Furthermore, we denote $(\cdot,\cdot) = \sum_{j=1}^{N} (\cdot,\cdot)_j$ and $\mathcal{H}^c = \sum_{j=1}^{N} \mathcal{H}^c_j$, $\mathcal{L}^{\pm} = \sum_{j=1}^{N} \mathcal{L}^{\pm}_j$. Then, summing the variational formulations (2.7) over all cells, we get the semi-discrete LDG scheme in the global form: find $\big(u(\cdot,t), p(\cdot,t), q(\cdot,t)\big) \in [V_h]^3$, such that

$$(u_t, v) = \mathcal{H}^c(f(u), v) - \mathcal{L}^+(p, v), \tag{2.8a}$$

$$(p, \phi) = -\mathcal{L}^-(q, \phi), \tag{2.8b}$$

$$(q, \psi) = -\mathcal{L}^-(u, \psi), \tag{2.8c}$$

hold for any test functions $v, \phi, \psi \in V_h$.

2.1.2 The semi-discrete LDG scheme for the wave equation (1.2)

Introducing four auxiliary variables $Z = U_x$, $O = Z_x$, $R = O_x$, $S = R_x$, we can rewrite (1.2) into the following equivalent first order system

$$U_t + f(U)_x - S_x = 0, \tag{2.9a}$$

$$S - R_x = 0, \tag{2.9b}$$

$$R - O_x = 0, \tag{2.9c}$$

$$O - Z_x = 0, \tag{2.9d}$$

$$Z - U_x = 0. \tag{2.9e}$$

The corresponding semi-discrete LDG scheme is defined as follows: find the map

$$\big(u(\cdot,t), z(\cdot,t), o(\cdot,t), r(\cdot,t), s(\cdot,t)\big) : [0,T] \to [V_h]^5,$$

such that

$$(u_t, v) = \mathcal{H}^c(f(u), v) - \mathcal{L}^+(s, v), \tag{2.10a}$$
$$(s, \phi) = -\mathcal{L}^-(r, \phi), \tag{2.10b}$$
$$(r, \zeta) = -\mathcal{L}^+(o, \zeta), \tag{2.10c}$$
$$(o, \varphi) = -\mathcal{L}^+(z, \varphi), \tag{2.10d}$$
$$(z, \psi) = -\mathcal{L}^-(u, \psi), \tag{2.10e}$$

hold for any test functions $v, \phi, \zeta, \varphi, \psi \in V_h$, where the definitions of $\mathcal{H}^c$ and $\mathcal{L}^\pm$ are the same as before.

2.1.3 Properties of the semi-discrete LDG schemes

The following elementary conclusions are cited from [39].

Lemma 2.1. *For any $w, v \in V_h$, there holds the equalities*

$$\mathcal{L}^\pm(w, v) + \mathcal{L}^\pm(v, w) = \pm\langle [\![w]\!], [\![v]\!] \rangle, \tag{2.11}$$
$$\mathcal{L}^\pm(v, v) = \pm\frac{1}{2}[\![v]\!]^2, \tag{2.12}$$
$$\mathcal{L}^-(w, v) + \mathcal{L}^+(v, w) = 0, \tag{2.13}$$

where $\langle [\![w]\!], [\![v]\!] \rangle = \sum_{j=1}^{N} [\![w]\!]_{j-\frac{1}{2}} [\![v]\!]_{j-\frac{1}{2}}$ and $[\![v]\!]^2 = \langle [\![v]\!], [\![v]\!] \rangle = \sum_{j=1}^{N} [\![v]\!]^2_{j-\frac{1}{2}}$.

A simple application of the above lemma leads to the following two corollaries, one can also refer to [26].

Corollary 2.1. *For any (u, q, p) satisfying (2.8b)-(2.8c), we have*

$$\mathcal{L}^+(p, u) = \frac{1}{2}[\![q]\!]^2. \tag{2.14}$$

Moreover, if both (u_1, q_1, p_1) and (u_2, q_2, p_2) satisfy (2.8b)-(2.8c), then

$$\mathcal{L}^+(p_1, u_2) + \mathcal{L}^+(p_2, u_1) = \langle [\![q_1]\!], [\![q_2]\!] \rangle. \tag{2.15}$$

Corollary 2.2. *For any (u, z, o, r, s) satisfying (2.10b)-(2.10e), we have*

$$\mathcal{L}^+(s, u) = \frac{1}{2}[\![o]\!]^2. \tag{2.16}$$

Moreover, if both $(u_1, z_1, o_1, r_1, s_1)$ and $(u_2, z_2, o_2, r_2, s_2)$ satisfy (2.10b)-(2.10e), then

$$\mathcal{L}^+(s_1, u_2) + \mathcal{L}^+(s_2, u_1) = \langle [\![o_1]\!], [\![o_2]\!] \rangle. \tag{2.17}$$

Based on the above corollaries, we can also derive the following lemma, which gives a deeper insight into the non-negative property of the operator $\mathcal{L}^+$, and one can refer to [35, Lemma 3.2] for the proof. It plays a key role in guiding us to construct semi-negative definite forms in the later analysis.

Lemma 2.2. *Denote* $\boldsymbol{w} = (w_1, \ldots, w_m)^\top$, $\boldsymbol{v} = (v_1, \ldots, v_m)^\top$, *where* m *is an arbitrary integer. Define*

$$\underline{\mathcal{L}}^+(\boldsymbol{w}, \boldsymbol{v}) = \sum_{i=1}^{m} \mathcal{L}^+(w_i, v_i). \tag{2.18}$$

Assume (u_i, q_i, p_i) *satisfy (2.8b)-(2.8c) and* $(u_i, z_i, o_i, r_i, s_i)$ *satisfy (2.10b)-(2.10e). Let* A *be a symmetric positive semi-definite matrix. We have*

$$\underline{\mathcal{L}}^+(\boldsymbol{p}, \mathsf{A}\boldsymbol{u}) \geq 0, \tag{2.19}$$

$$\underline{\mathcal{L}}^+(\boldsymbol{s}, \mathsf{A}\boldsymbol{u}) \geq 0, \tag{2.20}$$

where $\boldsymbol{p} = (p_1, \ldots, p_m)^\top$, $\boldsymbol{s} = (s_1, \ldots, s_m)^\top$ *and* $\boldsymbol{u} = (u_1, \ldots, u_m)^\top$.

2.2 Fully discrete schemes

We will adopt a third order IMEX-RK scheme in time discretization. Next we give a brief introduction of IMEX-RK schemes. For the detail introduction of IMEX-RK schemes, we refer to [10, 1, 7, 18, 25]. To introduce the IMEX-RK schemes, we consider the following ordinary differential systems

$$\frac{\mathrm{d}\mathbf{y}}{\mathrm{d}t} = L(t, \mathbf{y}) + N(t, \mathbf{y}), \qquad \mathbf{y}(t_0) = \mathbf{y}_0,$$

where $\mathbf{y} = [y_1, y_2, \cdots, y_d]^\top$, L and N are derived from the spatial discretization of the dispersion and the convection part, respectively. Assume we have obtained the solutions at time level t^n, denoted as $\mathbf{y}_n$; then the solutions at the next time level $t^{n+1} = t_n + \tau$ are given by the following ν-stage IMEX-RK time discretization scheme:

$$\begin{aligned}
&\mathbf{Y}_1 = \mathbf{y}_n, \\
&\mathbf{Y}_i = \mathbf{y}_n + \tau \sum_{j=2}^{i} a_{ij} L(t_n^j, \mathbf{Y}_j) + \tau \sum_{j=1}^{i-1} \hat{a}_{ij} N(t_n^j, \mathbf{Y}_j), \quad 2 \leq i \leq \nu + 1, \\
&\mathbf{y}_{n+1} = \mathbf{y}_n + \tau \sum_{i=2}^{\nu+1} b_i L(t_n^i, \mathbf{Y}_i) + \tau \sum_{i=1}^{\nu+1} \hat{b}_i N(t_n^i, \mathbf{Y}_i),
\end{aligned}$$

where $\mathbf{Y}_i$ stands for the solutions at the i-th intermediate stage, $c_i = \sum_{j=2}^{i} a_{ij} = \sum_{j=1}^{i-1} \hat{a}_{ij}$, and the intermediate time level $t_n^i = t_n + c_i\tau$ for $i \geq 2$. Usually, the above IMEX-RK scheme can be capped into the following Butcher tableau

$$\begin{array}{c|c|c}
\boldsymbol{c} & A & \hat{A} \\
\hline
 & \boldsymbol{b}^\top & \hat{\boldsymbol{b}}^\top
\end{array} \tag{2.21}$$

where both $A = (a_{ij})$ and $\hat{A} = (\hat{a}_{ij})$ are matrices of order $\nu+1$, $\boldsymbol{b}^\top = [0, b_2, \cdots, b_{\nu+1}]$, $\hat{\boldsymbol{b}}^\top = [\hat{b}_1, \cdots, \hat{b}_{\nu+1}]$ and $\boldsymbol{c}^\top = [0, c_2, \cdots, c_{\nu+1}]$. Note that in the above Butcher table, the left part and right part correspond to the implicit and explicit discretization, respectively. In this paper, we will consider a third order IMEX-RK scheme from [1] whose Butcher tableau is given below:

$$
\begin{array}{c|ccccc|ccccc}
0 & 0 & 0 & 0 & 0 & 0 & 0 & 0 & 0 & 0 & 0 \\
\frac{1}{2} & 0 & \frac{1}{2} & 0 & 0 & 0 & \frac{1}{2} & 0 & 0 & 0 & 0 \\
\frac{2}{3} & 0 & \frac{1}{6} & \frac{1}{2} & 0 & 0 & \frac{11}{18} & \frac{1}{18} & 0 & 0 & 0 \\
\frac{1}{2} & 0 & -\frac{1}{2} & \frac{1}{2} & \frac{1}{2} & 0 & \frac{5}{6} & -\frac{5}{6} & \frac{1}{2} & 0 & 0 \\
1 & 0 & \frac{3}{2} & -\frac{3}{2} & \frac{1}{2} & \frac{1}{2} & \frac{1}{4} & \frac{7}{4} & \frac{3}{4} & -\frac{7}{4} & 0 \\
\hline
 & 0 & \frac{3}{2} & -\frac{3}{2} & \frac{1}{2} & \frac{1}{2} & \frac{1}{4} & \frac{7}{4} & \frac{3}{4} & -\frac{7}{4} & 0
\end{array}
$$

The above scheme is stiffly accurate [6], when it coupled with the LDG schemes (2.8) and (2.10), the fully discrete schemes can be written as

$$(u^{n,\ell}, v) = (u^n, v) + \tau \sum_{i=0}^{\ell-1} c_{\ell i} \mathcal{H}^c(f(u^{n,i}), v) - \tau \sum_{i=0}^{\ell} d_{\ell i} \mathcal{L}^+(p^{n,i}, v), \tag{2.22a}$$

$$(p^{n,\ell}, \phi) = -\mathcal{L}^-(q^{n,\ell}, \phi), \tag{2.22b}$$

$$(q^{n,\ell}, \psi) = -\mathcal{L}^-(u^{n,\ell}, \psi), \tag{2.22c}$$

for the third order wave equation, and

$$(u^{n,\ell}, v) = (u^n, v) + \tau \sum_{i=0}^{\ell-1} c_{\ell i} \mathcal{H}^c(f(u^{n,i}), v) - \tau \sum_{i=0}^{\ell} d_{\ell i} \mathcal{L}^+(s^{n,i}, v), \tag{2.23a}$$

$$(s^{n,\ell}, \phi) = -\mathcal{L}^-(r^{n,\ell}, \phi), \tag{2.23b}$$

$$(r^{n,\ell}, \zeta) = -\mathcal{L}^+(o^{n,\ell}, \zeta), \tag{2.23c}$$

$$(o^{n,\ell}, \varphi) = -\mathcal{L}^+(z^{n,\ell}, \varphi), \tag{2.23d}$$

$$(z^{n,\ell}, \psi) = -\mathcal{L}^-(u^{n,\ell}, \psi), \tag{2.23e}$$

for the fifth order wave equation. In the above formulas, $\ell = 1, \ldots, 4$, $w^{n,0} = w^n$ and $w^{n,4} = w^{n+1}$ for $w = u, p, q, s, r, o, z$, and the coefficients of $c_{\ell i}$ and $d_{\ell i}$ are listed as follows

$c_{\ell i}$					$d_{\ell i}$				
1/2	0	0	0	0	0	1/2	0	0	0
11/18	1/18	0	0	0	0	1/6	1/2	0	0
5/6	-5/6	1/2	0	0	0	-1/2	1/2	1/2	0
1/4	7/4	3/4	-7/4	0	0	3/2	-3/2	1/2	1/2

As mentioned before, the energy stability analysis of the high order in time fully discrete IMEX-LDG schemes for the wave equations (1.1) and (1.2) are challenging, which is our long-term goal study. As a first step, in what follows we present the energy stability and error analysis for the purely implicit part, i.e., we consider the convection term $f(\cdot) = 0$. In this case, the fully discrete schemes (2.22) and (2.23) become purely implicit schemes.

3 Stability analysis

In this section, we present the stability analysis for the fully discrete IMEX-LDG schemes (2.22) and (2.23) with $f(\cdot)=0$. Our goal is to prove their unconditional stability. Since the proof line for the fifth order wave equation is almost the same as that for the third order wave equation, in what follows we only present the analysis for scheme (2.22) with $f(\cdot)=0$.

Theorem 3.1. *The schemes (2.22) and (2.23) with $f(\cdot)=0$ are unconditionally stable, namely, for any $\tau>0$, we have*

$$\|u^n\| \le \|u^0\| \quad \forall\ n. \tag{3.1}$$

Proof. Following the idea of [35] and the discussions in [24], we first define a series of temporal difference as follows

$$\begin{bmatrix} \mathbb{D}_0 w^n \\ \mathbb{D}_1 w^n \\ \mathbb{D}_2 w^n \\ \mathbb{D}_3 w^n \\ \mathbb{D}_4 w^n \end{bmatrix} = \begin{bmatrix} 1 & & & & \\ -2 & 2 & & & \\ 12 & -48 & 36 & & \\ 72 & -360 & 216 & 72 & \\ \frac{4896}{7} & -\frac{23616}{7} & \frac{15552}{7} & \frac{3456}{7} & -\frac{288}{7} \end{bmatrix} \begin{bmatrix} w^n \\ w^{n,1} \\ w^{n,2} \\ w^{n,3} \\ w^{n+1} \end{bmatrix}, \tag{3.2}$$

for $w=u,p,q$. It can be checked that (see [24])

$$w^{n+1} = w^n + \sum_{\ell=1}^{4} \omega_\ell \mathbb{D}_\ell w^n, \tag{3.3}$$

where

$$\omega_1 = 1, \quad \omega_2 = \frac{1}{2}, \quad \omega_3 = \frac{1}{6}, \quad \omega_4 = -\frac{7}{288}. \tag{3.4}$$

Taking L^2 norm on both sides of (3.3) with $w=u$ yields

$$\begin{aligned} &\|u^{n+1}\|^2 - \|u^n\|^2 \\ =&\sum_{\ell=1}^{4} \Big(\omega_\ell^2 \|\mathbb{D}_\ell u^n\|^2 + 2\omega_\ell (\mathbb{D}_\ell u^n, \mathbb{D}_0 u^n) \Big) + 2 \sum_{1\le i<\ell\le 4} \omega_i \omega_\ell (\mathbb{D}_\ell u^n, \mathbb{D}_i u^n) \\ \doteq& \mathcal{RHS}(u^n). \end{aligned} \tag{3.5}$$

However, we can not use this form of $\mathcal{RHS}(u^n)$ directly to derive the stability of the fully discrete scheme, since no spatial information was reflected. So we transfer it to spatial information with the aid of the following formulas which are obtained directly from the scheme (2.22):

$$(\mathbb{D}_\ell u^n, v) = -\tau \mathcal{L}^+(\mathbb{F}_\ell p^n, v), \tag{3.6a}$$

$$(\mathbb{D}_\ell p^n, \phi) = -\mathcal{L}^-(\mathbb{D}_\ell q^n, \phi), \tag{3.6b}$$

$$(\mathbb{D}_\ell q^n, \psi) = -\mathcal{L}^-(\mathbb{D}_\ell u^n, \psi), \tag{3.6c}$$

for $\ell = 1, \ldots, 4$. Here we adopt the short notations

$$\begin{bmatrix} \mathbb{F}_1 w^n \\ \mathbb{F}_2 w^n \\ \mathbb{F}_3 w^n \\ \mathbb{F}_4 w^n \end{bmatrix} = \mathsf{F} \boldsymbol{w^n}, \tag{3.7}$$

with

$$\mathsf{F} = \begin{bmatrix} 1 & \frac{1}{2} & 0 & 0 & 0 \\ 0 & 3 & \frac{1}{2} & 0 & 0 \\ 0 & 24 & 1 & \frac{1}{2} & 0 \\ 0 & \frac{1584}{7} & \frac{72}{7} & -\frac{2}{7} & \frac{1}{2} \end{bmatrix} \quad \text{and} \quad \boldsymbol{w^n} = \begin{bmatrix} \mathbb{D}_0 w^n \\ \mathbb{D}_1 w^n \\ \mathbb{D}_2 w^n \\ \mathbb{D}_3 w^n \\ \mathbb{D}_4 w^n \end{bmatrix}, \tag{3.8}$$

for $w = u, p, q$.

Let us now turn back to the estimate for $\mathcal{RHS}(u^n)$. In order to obtain the unconditional stability result (3.1), we need to prove $\mathcal{RHS}(u^n)$ is non-positive. Our main idea is to transfer $\mathcal{RHS}(u^n)$ to spatial information and to construct a semi-negative definite symmetric form. However, if we transfer all the terms in $\mathcal{RHS}(u^n)$ to the information of the spatial discretization, then we cannot get the desired result. Thus, to have more degree of freedom to construct the semi-negative definite symmetric form, we leave some terms alone and just transfer part of the terms in $\mathcal{RHS}(u^n)$. Specifically, we introduce some undetermined parameters $\{\delta_\ell\}_{\ell=1}^7$ to split $\mathcal{RHS}(u^n)$ into two parts as follows:

$$\mathcal{RHS}(u^n) = \mathcal{RT}(u^n) + \mathcal{RS}(u^n), \tag{3.9}$$

where

$$\mathcal{RT}(u^n) = \sum_{\ell=1}^{4} \delta_\ell \|\mathbb{D}_\ell u^n\|^2 + \delta_5(\mathbb{D}_3 u^n, \mathbb{D}_2 u^n) + \delta_6(\mathbb{D}_4 u^n, \mathbb{D}_2 u^n) + \delta_7(\mathbb{D}_4 u^n, \mathbb{D}_3 u^n),$$

and $\mathcal{RS}(u^n)$ contains the remaining terms, i.e.,

$$\begin{aligned} \mathcal{RS}(u^n) = \sum_{\ell=1}^{4} \Big((\omega_\ell^2 - \delta_\ell) \|\mathbb{D}_\ell u^n\|^2 + 2\omega_\ell (\mathbb{D}_\ell u^n, \mathbb{D}_0 u^n) \Big) \\ + 2\omega_1\omega_2 (\mathbb{D}_1 u^n, \mathbb{D}_2 u^n) + 2\omega_1\omega_3 (\mathbb{D}_1 u^n, \mathbb{D}_3 u^n) \\ + 2\omega_1\omega_4 (\mathbb{D}_1 u^n, \mathbb{D}_4 u^n) + (2\omega_2\omega_3 - \delta_5)(\mathbb{D}_2 u^n, \mathbb{D}_3 u^n) \\ + (2\omega_2\omega_4 - \delta_6)(\mathbb{D}_2 u^n, \mathbb{D}_4 u^n) + (2\omega_3\omega_4 - \delta_7)(\mathbb{D}_3 u^n, \mathbb{D}_4 u^n). \end{aligned}$$

The terms in $\mathcal{RS}(u^n)$ will be converted to spatial discretization and hopefully a semi-negative definite symmetric form can be constructed. Meanwhile, we hope the terms in $\mathcal{RT}(u^n)$ can be written as a quadratic form about the temporal differences which is also semi-negative.

Then, for the purpose of exploiting (3.6a) to construct symmetric forms, we further

introduce undetermined parameters $\{\alpha_\ell\}_{\ell=1}^6$ to express $\mathcal{RS}(u^n)$ as

$$\begin{aligned}\mathcal{RS}(u^n) = &\sum_{\ell=1}^{4}\Big((\omega_\ell^2-\delta_\ell)\|\mathbb{D}_\ell u^n\|^2 + 2\omega_\ell(\mathbb{D}_\ell u^n, \mathbb{D}_0 u^n)\Big)\\ &+\alpha_1(\mathbb{D}_2u^n,\mathbb{D}_1u^n)+\alpha_2(\mathbb{D}_3u^n,\mathbb{D}_1u^n)+\alpha_3(\mathbb{D}_4u^n,\mathbb{D}_1u^n)\\ &+\alpha_4(\mathbb{D}_3u^n,\mathbb{D}_2u^n)+\alpha_5(\mathbb{D}_4u^n,\mathbb{D}_2u^n)+\alpha_6(\mathbb{D}_4u^n,\mathbb{D}_3u^n)\\ &+(2\omega_1\omega_2-\alpha_1)(\mathbb{D}_1u^n,\mathbb{D}_2u^n)+(2\omega_1\omega_3-\alpha_2)(\mathbb{D}_1u^n,\mathbb{D}_3u^n)\\ &+(2\omega_1\omega_4-\alpha_3)(\mathbb{D}_1u^n,\mathbb{D}_4u^n)+(2\omega_2\omega_3-\alpha_4-\delta_5)(\mathbb{D}_2u^n,\mathbb{D}_3u^n)\\ &+(2\omega_2\omega_4-\alpha_5-\delta_6)(\mathbb{D}_2u^n,\mathbb{D}_4u^n)+(2\omega_3\omega_4-\alpha_6-\delta_7)(\mathbb{D}_3u^n,\mathbb{D}_4u^n).\end{aligned}$$

Note that the above expression can be also expressed as

$$\mathcal{RS}(u^n) = \sum_{\ell=1}^{4}(\mathbb{D}_\ell u^n, \mathbb{E}_\ell u^n), \tag{3.10}$$

where

$$\begin{bmatrix}\mathbb{E}_1 w^n\\ \mathbb{E}_2 w^n\\ \mathbb{E}_3 w^n\\ \mathbb{E}_4 w^n\end{bmatrix} = \mathsf{E}\boldsymbol{w^n}, \tag{3.11}$$

with

$$\mathsf{E} = \begin{bmatrix}2\omega_1 & \omega_1^2-\delta_1 & 2\omega_1\omega_2-\alpha_1 & 2\omega_1\omega_3-\alpha_2 & 2\omega_1\omega_4-\alpha_3\\ 2\omega_2 & \alpha_1 & \omega_2^2-\delta_2 & 2\omega_2\omega_3-\alpha_4-\delta_5 & 2\omega_2\omega_4-\alpha_5-\delta_6\\ 2\omega_3 & \alpha_2 & \alpha_4 & \omega_3^2-\delta_3 & 2\omega_3\omega_4-\alpha_6-\delta_7\\ 2\omega_4 & \alpha_3 & \alpha_5 & \alpha_6 & \omega_4^2-\delta_4\end{bmatrix},$$

and $\boldsymbol{w^n}$ being defined in (3.8).

In what follows, we will determine the above parameters $\{\delta_\ell\}_{\ell=1}^7$ and $\{\alpha_\ell\}_{\ell=1}^6$. Starting from (3.10) and (3.6a), we get

$$\begin{aligned}\mathcal{RS}(u^n) &= -\tau\sum_{\ell=1}^{4}\mathcal{L}^+(\mathbb{F}_\ell p^n, \mathbb{E}_\ell u^n)\\ &= -\tau\underline{\mathcal{L}}^+(\mathsf{F}\boldsymbol{p^n}, \mathsf{E}\boldsymbol{u^n})\\ &= -\tau\underline{\mathcal{L}}^+(\boldsymbol{p^n}, \mathsf{F}^\top\mathsf{E}\boldsymbol{u^n}).\end{aligned} \tag{3.12}$$

In the above formula, the second step holds by the definition (2.18), and the last step holds by noting that $(\mathsf{F}\boldsymbol{p^n})^\top\mathsf{E}\boldsymbol{u^n} = (\boldsymbol{p^n})^\top\mathsf{F}^\top\mathsf{E}\boldsymbol{u^n}$. So according to Lemma 2.2, the requirement of $\mathcal{RS}(u^n)\le 0$ can be ensured if the matrix $\mathsf{F}^\top\mathsf{E}$ is symmetric positive semi-definite. Since $\mathsf{F}^\top\mathsf{E}$ is a 5×5 matrix, the requirement of symmetric will lead to a linear system of 10 equations with 13 unknowns $\{\delta_\ell\}_{\ell=1}^7$ and $\{\alpha_\ell\}_{\ell=1}^6$. Apparently, the solution of this system

is not unique. Solving the system by Maple, we can get one solution

$$\begin{aligned}
&\delta_1 = 0,\ \alpha_1 = \frac{2}{3},\ \alpha_2 = \frac{11}{72},\ \alpha_3 = -\frac{7}{288},\\
&\delta_2 = \frac{4679}{72} + 48\delta_3 + \frac{107808}{7}\alpha_6 + 8160\delta_7,\ \delta_4 = \frac{1225}{82944} + \frac{7}{2}\alpha_6 + \frac{7}{4}\delta_7,\\
&\delta_5 = \frac{19}{216} - 14\delta_3 + \frac{120}{7}\alpha_6 - \frac{408}{7}\delta_7,\ \delta_6 = -\frac{1715}{864} - 470\alpha_6 - 242\delta_7,\\
&\alpha_4 = \frac{131}{432} + 6\delta_3 + \frac{408}{7}\alpha_6 + \frac{408}{7}\delta_7,\ \alpha_5 = \frac{119}{144} + 198\alpha_6 + 102\delta_7.
\end{aligned}$$

Note that there are three free parameters $\delta_3, \delta_7, \alpha_6$ in this solution. We can choose proper values to meet our requirements that $\mathcal{RS}(u^n) \le 0$ and $\mathcal{RT}(u^n) \le 0$. The choice of the desired free parameters is not unique. For instance, we can take

$$\delta_3 = -\frac{1}{10},\ \delta_7 = \frac{62064468034163}{2944944650419200},\ \alpha_6 = -\frac{2029867}{134576640}. \tag{3.13}$$

This choice will lead to a negative definite matrix

$$\mathsf{T} = \begin{bmatrix} \delta_2 & \delta_5/2 & \delta_6/2 \\ & \delta_3 & \delta_7/2 \\ sym & & \delta_4 \end{bmatrix}.$$

Note that $\delta_1 = 0$, thus the term $\mathcal{RT}(u^n)$ can be expressed into a non-positive quadratic form, namely

$$\mathcal{RT}(u^n) = \int_\Omega [\mathbb{D}_2 u^n, \mathbb{D}_3 u^n, \mathbb{D}_4 u^n]\mathsf{T}[\mathbb{D}_2 u^n, \mathbb{D}_3 u^n, \mathbb{D}_4 u^n]^\top dx \le 0, \tag{3.14}$$

since T is negative definite. Moreover, the choice (3.13) also leads to a positive semi-definite matrix $\mathsf{F}^\top\mathsf{E}$ whose smallest non-negative eigenvalue is 0, and thus

$$\mathcal{RS}(u^n) \le 0. \tag{3.15}$$

Hence, we get $\|u^{n+1}\| \le \|u^n\| \le \cdots \|u^0\|$ and complete the proof of this theorem. □

Remark 3.1. We remark that $\mathcal{RT}(u^n) \le 0$ is enough for our stability analysis, but for the convenience of error estimates in the next section, we further need the estimate

$$\mathcal{RT}(u^n) \le \lambda \sum_{\ell=2}^{4} \|\mathbb{D}_\ell u^n\|^2, \tag{3.16}$$

where $\lambda \approx -4.9525 * 10^{-7}$ is the largest negative eigenvalue of the matrix T.

Remark 3.2. The proof of scheme (2.23) with $f(\cdot) = 0$ for the fifth order wave equation is similar. The splitting of $\mathcal{RHS}(u^n) = \mathcal{RT}(u^n) + \mathcal{RS}(u^n)$ is the same as above, the only difference is $\mathcal{RS}(u^n) = -\tau\underline{\mathcal{L}}^+(\boldsymbol{s^n}, \mathsf{F}^\top\mathsf{E}\boldsymbol{u^n})$, where $\boldsymbol{s^n} = (\mathbb{D}_0 s^n, \mathbb{D}_1 s^n, \mathbb{D}_2 s^n, \mathbb{D}_3 s^n, \mathbb{D}_4 s^n)^\top$. By Lemma 2.2 we also have $\mathcal{RS}(u^n) \le 0$. Thus (3.1) can be obtained.

Remark 3.3. According to [24], we know that the temporal difference defined in (3.2) uses the explicit part of the IMEX-RK scheme, i.e., they satisfy the following relationship

$$(\mathbb{D}_\ell u^n, v) = \tau \mathcal{H}^c(\mathbb{D}_{\ell-1} u^n, v), \qquad v \in V_h,$$

if the convection term $f(U) = U$ and the third/fifth order derivative terms vanish. Hence, the technique might be helpful for our future study on the stability of the corresponding schemes for (1.1) and (1.2) with the convection flux $f(U) \neq 0$.

4 Error estimates

In this section, we will take the third order wave equation as an example to show the optimal error estimates for the scheme (2.22). Optimal error estimates of the scheme (2.23) for the fifth order wave equation can be obtained similarly. In this section, we still consider $f(\cdot) = 0$.

The projection technique proposed in [26] will play a crucial rule in the error estimates. Let $U(x)$ be a given function satisfying the periodic boundary condition, we denote $\boldsymbol{W} = (U, P, Q)$ with $Q = U_x$ and $P = Q_x$. Their projection $\boldsymbol{W}_h = (U_h, P_h, Q_h)$ is defined as follows

$$\mathcal{L}^+(P, v) = \mathcal{L}^+(P_h, v), \quad \forall v \in V_h, \tag{4.1a}$$
$$(P_h, \phi) = -\mathcal{L}^-(Q_h, \phi), \quad \forall \phi \in V_h, \tag{4.1b}$$
$$(Q_h, \psi) = -\mathcal{L}^-(U_h, \psi), \quad \forall \psi \in V_h. \tag{4.1c}$$

Moreover, to ensure the uniqueness of $\boldsymbol{W}_h$, we require

$$(P_h, 1) = (Q_h, 1) = (U - U_h, 1) = 0. \tag{4.1d}$$

From the discussion in [26], we have the following lemma for the projection $\boldsymbol{W}_h$:

Lemma 4.1. *[26, Lemma 4.3] The projection $\boldsymbol{W}_h$ defined in (4.1) exists uniquely and satisfies the following optimal approximation property*

$$\|U_h - U\| + \|P_h - P\| + \|Q_h - Q\| \leq C h^{k+1}, \tag{4.2}$$

where C depends on the regularity of U, which is assumed to be in $H^{k+3}(\Omega)$.

By the aid of the above projection and along the similar argument as the stability analysis, we can obtain the following theorem. Before presenting the main result about the error estimates, we give the definition of the initial values, which are taken as the projection of (U_0, P_0, Q_0) defined in (4.1), namely

$$(u^0, p^0, q^0) = (U_h^0, P_h^0, Q_h^0), \tag{4.3}$$

where U_0 is the given initial condition, $Q_0 = U_0'$ and $P_0 = U_0''$.

Theorem 4.1. *Let u^n be the numerical solution of scheme (2.22) with $f(\cdot)=0$, with the initial solution (4.3). Let $U(x,t)$ be the exact solution of (1.1) with $f(U)=0$ and denote $U^n=U(x,t^n)$. Assume $U(x,t)$ is sufficiently smooth such that*

$$U, U_t \in L^\infty(H^{k+3}) \quad \textit{and} \quad U_t^{(4)} \in L^\infty(L^2). \tag{4.4}$$

Then there exists a positive constant τ_0 which is independent of the mesh size h, such that for $\tau \le \tau_0$, we have

$$\|U^n - u^n\| \le C(h^{k+1}+\tau^3) \quad \forall\ n \ge 0, \tag{4.5}$$

where $C>0$ is the bounding constant independent of h and τ.

Proof. Denote $\boldsymbol{W}^{n,\ell}=(U^{n,\ell},P^{n,\ell},Q^{n,\ell})$ as the exact solution of (2.2) with $f(U)=0$ at time level $t^{n,\ell}$ and denote the errors as

$$\boldsymbol{e}^{n,\ell}=(e_u^{n,\ell},e_p^{n,\ell},e_q^{n,\ell})=(U^{n,\ell}-u^{n,\ell},P^{n,\ell}-p^{n,\ell},Q^{n,\ell}-q^{n,\ell})=\boldsymbol{W}^{n,\ell}-\boldsymbol{w}^{n,\ell}. \tag{4.6}$$

With the help of the projection $\boldsymbol{W}_h$, we divide the errors into the form $\boldsymbol{e}^{n,\ell}=\boldsymbol{\xi}^{n,\ell}-\boldsymbol{\eta}^{n,\ell}$, with

$$\boldsymbol{\xi}^{n,\ell}=\boldsymbol{W}_h^{n,\ell}-\boldsymbol{w}^{n,\ell}, \quad \boldsymbol{\eta}^{n,\ell}=\boldsymbol{W}_h^{n,\ell}-\boldsymbol{W}^{n,\ell}.$$

From the definition of the projection $\boldsymbol{W}_h$, we have the following equalities

$$0=\mathcal{L}^+(\eta_p^{n,\ell},v), \quad (\eta_p^{n,\ell},\phi)=-\mathcal{L}^-(\eta_q^{n,\ell},\phi), \quad (\eta_q^{n,\ell},\psi)=-\mathcal{L}^-(\eta_u^{n,\ell},\psi). \tag{4.7}$$

Moreover, since the projection $\boldsymbol{W}_h$ is linear, from (4.2) we can derive that

$$\|\mathbb{D}_\ell \eta_u^n\| \le Ch^{k+1}\tau, \tag{4.8}$$

where the constant C depends on $\|U_t\|_{H^{k+3}}$. In what follows we will estimate $\boldsymbol{\xi}$. The process starts from the error equations as to be established below.

Since the exact solution is smooth enough, we get that $\boldsymbol{W}^{n,\ell}$ satisfy the following variational forms:

$$(\mathbb{D}_\ell U^n,v) = -\tau\mathcal{L}^+(\mathbb{F}_\ell P^n,v)+(\kappa_{4\ell}\varsigma^n,v), \quad \forall v\in V_h, \tag{4.9a}$$
$$(\mathbb{D}_\ell P^n,\phi) = -\mathcal{L}^-(\mathbb{D}_\ell Q^n,\phi), \quad \forall \phi\in V_h, \tag{4.9b}$$
$$(\mathbb{D}_\ell Q^n,\psi) = -\mathcal{L}^-(\mathbb{D}_\ell U^n,\psi), \quad \forall \psi\in V_h. \tag{4.9c}$$

Here $\kappa_{4\ell}=0$ for $\ell=1,2,3$ and $\kappa_{4\ell}=1$ for $\ell=4$, ς^n is the local truncation error satisfying

$$\|\varsigma^n\| \le C\tau^4, \tag{4.10}$$

with a positive constant C depending on $\|U_t^{(4)}\|_{L^\infty(L^2)}$.

Then, subtracting (2.22) from (4.9) and by (4.7), we get the following error equations

$$(\mathbb{D}_\ell \xi_u^n,v) = (\mathbb{D}_\ell\eta_u^n+\kappa_{4\ell}\varsigma^n,v)-\tau\mathcal{L}^+(\mathbb{F}_\ell\xi_p^n,v), \tag{4.11a}$$
$$(\mathbb{D}_\ell \xi_p^n,\phi) = -\mathcal{L}^-(\mathbb{D}_\ell\xi_q^n,\phi), \tag{4.11b}$$
$$(\mathbb{D}_\ell \xi_q^n,\psi) = -\mathcal{L}^-(\mathbb{D}_\ell\xi_u^n,\psi), \tag{4.11c}$$

for any test functions $v, \phi, \psi \in V_h$.

Comparing with (2.22), there are only two extra terms relating the projection and the local truncation error in the error equations (4.11). Hence, along the similar procedure as the stability analysis, we have

$$\|\xi_u^{n+1}\|^2 - \|\xi_u^n\|^2 = \mathcal{RT}(\xi_u^n) + \mathcal{RS}(\xi_u^n), \tag{4.12}$$

where $\mathcal{RT}(\xi_u^n)$ and $\mathcal{RS}(\xi_u^n)$ are defined in the same way as $\mathcal{RT}(u^n)$ and $\mathcal{RS}(u^n)$, the only change is replacing u with ξ_u. The parameters $\{\delta_\ell\}_{\ell=1}^7$ and $\{\alpha_\ell\}_{\ell=1}^6$ are the same as before.

As the discussions in Remark 3.1, we can get

$$\mathcal{RT}(\xi_u^n) \le \lambda \sum_{\ell=2}^{4} \|\mathbb{D}_\ell \xi_u^n\|^2, \tag{4.13}$$

where $\lambda \approx -4.9525 * 10^{-7}$ is the largest negative eigenvalue of the matrix T. Similar to (3.10), we have

$$\begin{aligned} \mathcal{RS}(\xi_u^n) &= \sum_{\ell=1}^{4} (\mathbb{D}_\ell \xi_u^n, \mathbb{E}_\ell \xi_u^n) \\ &= \sum_{\ell=1}^{4} (\mathbb{D}_\ell \eta_u^n + \kappa_{4\ell} \varsigma^n, \mathbb{E}_\ell \xi_u^n) - \tau \sum_{\ell=1}^{4} \mathcal{L}^+(\mathbb{F}_\ell \xi_u^n, \mathbb{E}_\ell \xi_u^n) \\ &\doteq \Lambda_1 + \Lambda_2, \end{aligned} \tag{4.14}$$

where in the second step we used (4.11a). Similar to the estimate for $\mathcal{RS}(u^n)$ in (3.12), we have

$$\Lambda_2 \le 0. \tag{4.15}$$

By the Cauchy-Schwarz inequality, the properties (4.8) and (4.10), and the relationships between $\mathbb{E}_\ell$ and $\mathbb{D}_\ell$ (see the definition in (3.11)), we can easily get

$$\Lambda_1 \le C(h^{k+1}\tau + \tau^4) \sum_{\ell=1}^{4} \|\mathbb{E}_\ell \xi_u^n\| \le C(h^{k+1}\tau + \tau^4) \sum_{\ell=0}^{4} \|\mathbb{D}_\ell \xi_u^n\|. \tag{4.16}$$

By the relationship (3.3), we can express $\mathbb{D}_1 \xi_u^n$ as $\mathbb{D}_1 \xi_u^n = \xi_u^{n+1} - \xi_u^n - \sum_{\ell=2}^{4} \omega_\ell \mathbb{D}_\ell \xi_u^n$. Then using the Young inequality, we obtain

$$\Lambda_1 \le \tau(\|\xi_u^n\|^2 + \|\xi_u^{n+1}\|^2) + \varepsilon \sum_{\ell=2}^{4} \|\mathbb{D}_\ell \xi_u^n\|^2 + C(h^{2k+2}\tau + \tau^7), \tag{4.17}$$

where ε is any positive constant. Taking $\varepsilon = -\lambda$, we get

$$\|\xi_u^{n+1}\|^2 - \|\xi_u^n\|^2 \le \tau(\|\xi_u^n\|^2 + \|\xi_u^{n+1}\|^2) + C(h^{2k+2}\tau + \tau^7). \tag{4.18}$$

Then there exists a constant $\tilde{C} > 2$ such that

$$\begin{aligned} \|\xi_u^{n+1}\|^2 &\le \frac{1+\tau}{1-\tau} \|\xi_u^n\|^2 + C(h^{2k+2}\tau + \tau^7) \\ &\le (1 + \tilde{C}\tau)\|\xi_u^n\|^2 + C(h^{2k+2}\tau + \tau^7), \end{aligned} \tag{4.19}$$

if $\tau \leq \frac{\tilde{C}-2}{\tilde{C}}$. Finally, by the discrete Gronwall inequality, we can directly get

$$\|\xi_u^n\|^2 \leq e^{\tilde{C}n\tau}\|\xi_u^0\|^2 + C(h^{2k+2} + \tau^6). \tag{4.20}$$

By the choice of initial value (4.3), we have $\xi_u^0 = 0$. Hence,

$$\|\xi_u^n\| \leq C(h^{k+1} + \tau^3). \tag{4.21}$$

Then by the triangle inequality and (4.2), we get the conclusion of this theorem. □

Remark 4.1. The optimal error estimates for the fifth order wave equation can be obtained by defining a similar projection as (4.1). To be specific, for function $U(x)$ satisfying the periodic boundary condition, we denote $\boldsymbol{G} = (U, Z, O, R, S)$ with $Z = U_x, O = Z_x, R = O_x, S = R_x$. Their projection $\boldsymbol{G}_h = (U_h, Z_h, O_h, R_h, S_h)$ is defined as follows

$$\begin{aligned}
\mathcal{L}^+(S, v) &= \mathcal{L}^+(S_h, v), && \forall v \in V_h, && \text{(4.22a)}\\
(S_h, \phi) &= -\mathcal{L}^-(R_h, \phi), && \forall \phi \in V_h, && \text{(4.22b)}\\
(R_h, \zeta) &= -\mathcal{L}^+(O_h, \zeta), && \forall \zeta \in V_h, && \text{(4.22c)}\\
(O_h, \varphi) &= -\mathcal{L}^+(Z_h, \varphi), && \forall \varphi \in V_h, && \text{(4.22d)}\\
(Z_h, \psi) &= -\mathcal{L}^-(O_h, \psi), && \forall \psi \in V_h. && \text{(4.22e)}
\end{aligned}$$

Moreover, to ensure the uniqueness of $\boldsymbol{G}_h$, we require

$$(S_h, 1) = (R_h, 1) = (O_h, 1) = (Z_h, 1) = (U - U_h, 1) = 0. \tag{4.22f}$$

Along the similar arguments as that for the projection $\boldsymbol{W}_h$ in [26], we can also obtain the optimal approximation property for the projection $\boldsymbol{G}_h$.

5 Numerical experiments

Even though only the theoretical analysis for schemes (2.22) and (2.23) with $f(\cdot) = 0$ was presented, in this section we will give numerical experiments for both the cases $f(\cdot) = 0$ and $f(\cdot) \neq 0$. Numerical tests will be carried out to verify the accuracy and performance of schemes (2.22) and (2.23) for the third order and the fifth order wave equations, respectively. In the spatial discretization, we will adopt piecewise second order polynomials. In all experiments, only the highest order term is treated implicitly in time discretization, and other terms are treated explicitly. For the cases with linear/nonlinear convection term, we take upwind/Lax-Friedrichs flux for this term. Besides, we will adopt uniform meshes in all the experiments.

5.1 Numerical test for the third order equation

Example 5.1. In this example, we consider the linear third order KdV equation

$$U_t + cU_x = dU_{xxx}, \quad (x, t) \in [0, 2\pi] \times (0, T], \tag{5.1}$$

the initial condition is $U_0(x) = \sin(x)$ and the exact solution is $U(x, t) = \sin\big(x - (c + d)t\big)$. We display in Table 1 the L^2 errors and orders of accuracy for this example with $d = 1$ and different values of $c = 0, 2, 5, 10$. The final computing time is $T = 1$ and the time step is taken as $\tau = 0.5h$. From the table, we observe optimal error accuracy.

Table 1: The L^2 errors and orders of accuracy for equation (5.1) with $d = 1$ and different values of c. $T = 1$, $\tau = 0.5h$.

N	$c = 0$		$c = 2$		$c = 5$		$c = 10$	
	L^2 error	order	L^2 error	order	L^2 error	order	L^2 error	order
40	5.33E-05	-	1.75E-03	-	5.30E-02	-	7.17E-01	-
80	6.69E-06	2.99	2.24E-04	2.97	6.82E-03	2.96	1.01E-01	2.82
160	8.39E-07	3.00	2.84E-05	2.98	8.65E-04	2.98	1.31E-02	2.96
320	1.05E-07	3.00	3.55E-06	3.00	1.08E-04	3.00	1.64E-03	3.00
640	1.31E-08	3.00	4.44E-07	3.00	1.35E-05	3.00	2.05E-04	3.00

Example 5.2. In this example, we consider the nonlinear KdV equation

$$U_t + (3U^2)_x + U_{xxx} = 0, \tag{5.2}$$

with the exact solution $U(x,t) = \frac{1}{2}\text{sech}^2\left(\frac{1}{2}(x-t)\right)$. The computational domain is taken as $[-25, 25]$. The final computing time is $T = 1$ and the time step is $\tau = 0.1h$. The results are listed in Table 2, from which we can see optimal error accuracy.

Table 2: The L^2 errors and orders of accuracy for equation (5.2). $T = 1$, $\tau = 0.1h$.

N	40	80	160	320	640
L^2 error	5.69E-03	7.05E-04	8.86E-05	1.11E-05	1.39E-06
order	-	3.01	2.99	3.00	3.00

Example 5.3. We compute the classical soliton solutions of the KdV equation

$$U_t + (U^2/2)_x + dU_{xxx} = 0. \tag{5.3}$$

In this example, we take $N = 160$ and $\tau = 0.01$. The following cases were also tested in [13, 37].

(i). The single soliton case has the initial condition $U_0(x) = 3\Lambda\text{sech}^2(\kappa(x - x_0))$, where $\Lambda = 0.3$, $x_0 = 0.5$, $\kappa = \frac{1}{2}\sqrt{\frac{\Lambda}{d}}$ and $d = 5 \times 10^{-4}$. The exact solution is

$$U(x,t) = 3\Lambda\text{sech}^2(\kappa(x - x_0 - \Lambda t)). \tag{5.4}$$

The numerical solution is computed in $[0, 2]$. We display the exact and numerical solutions at time $T = 0, 1, 2, 3$ in Figure 1, from which we find that the numerical solutions coincide well with the exact solutions.

(ii). The double soliton collision case has the initial condition

$$U_0(x) = 3\Lambda_1\text{sech}^2(\kappa_1(x - x_1)) + 3\Lambda_2\text{sech}^2(\kappa_2(x - x_2)),$$

where $\Lambda_1 = 0.3$, $\Lambda_2 = 0.1$, $x_1 = 0.4$, $x_2 = 0.8$, $\kappa_i = \frac{1}{2}\sqrt{\frac{\Lambda_i}{d}}$ for $i = 1, 2$ and $d = 4.84 \times 10^{-4}$. The numerical solution is also computed in $[0, 2]$ and the results at time $T = 0, 1, 2, 3$ are shown in Figure 2.

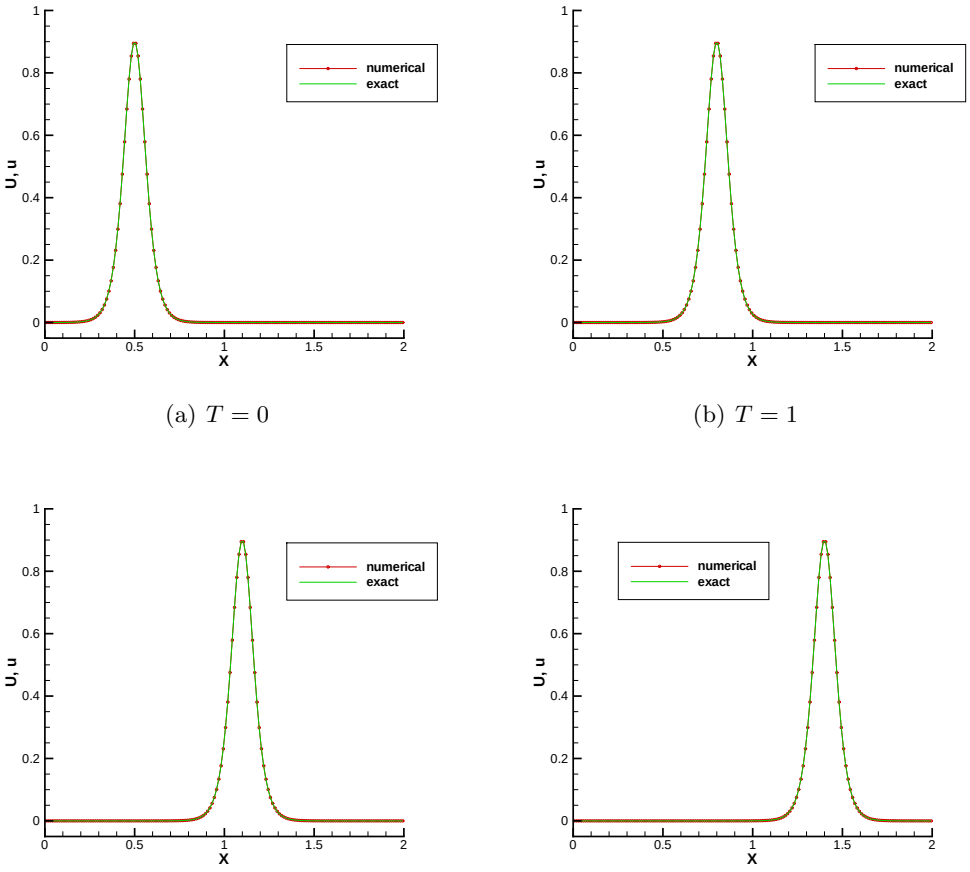

(a) $T = 0$ (b) $T = 1$

(c) $T = 2$ (d) $T = 3$

Figure 1: Example 5.3 (i): Single soliton profiles at time $T = 0, 1, 2, 3$.

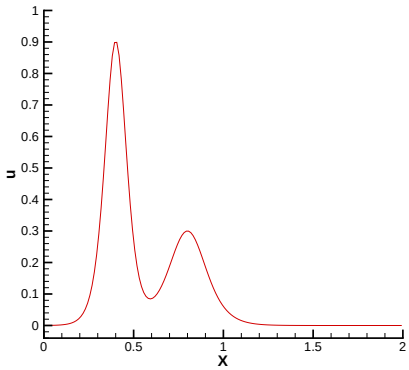

(a) $T = 0$

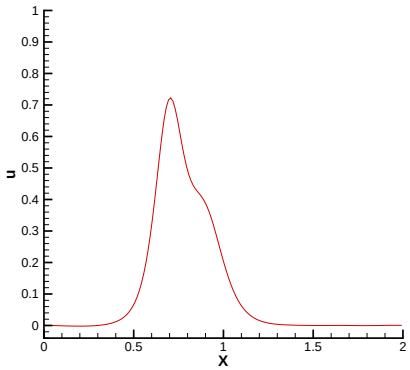

(b) $T = 1$

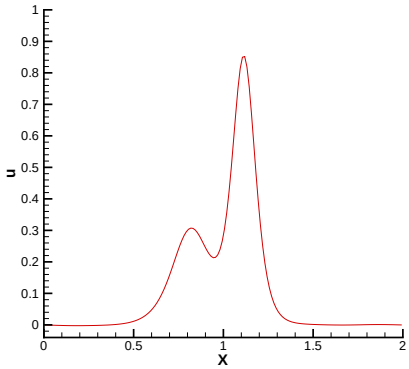

(c) $T = 2$

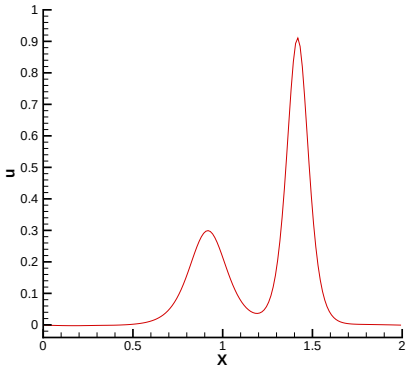

(d) $T = 3$

Figure 2: Example 5.3 (ii): Double soliton collision profiles at time $T = 0, 1, 2, 3$.

(iii). The triple soliton splitting case has the initial condition $U_0(x) = \frac{2}{3}\text{sech}^2((x-1)/\sqrt{108d})$ with $d = 10^{-4}$. The numerical solution is computed in $[0, 3]$ and the results at time $T = 0, 1, 2, 3$ are displayed in Figure 3.

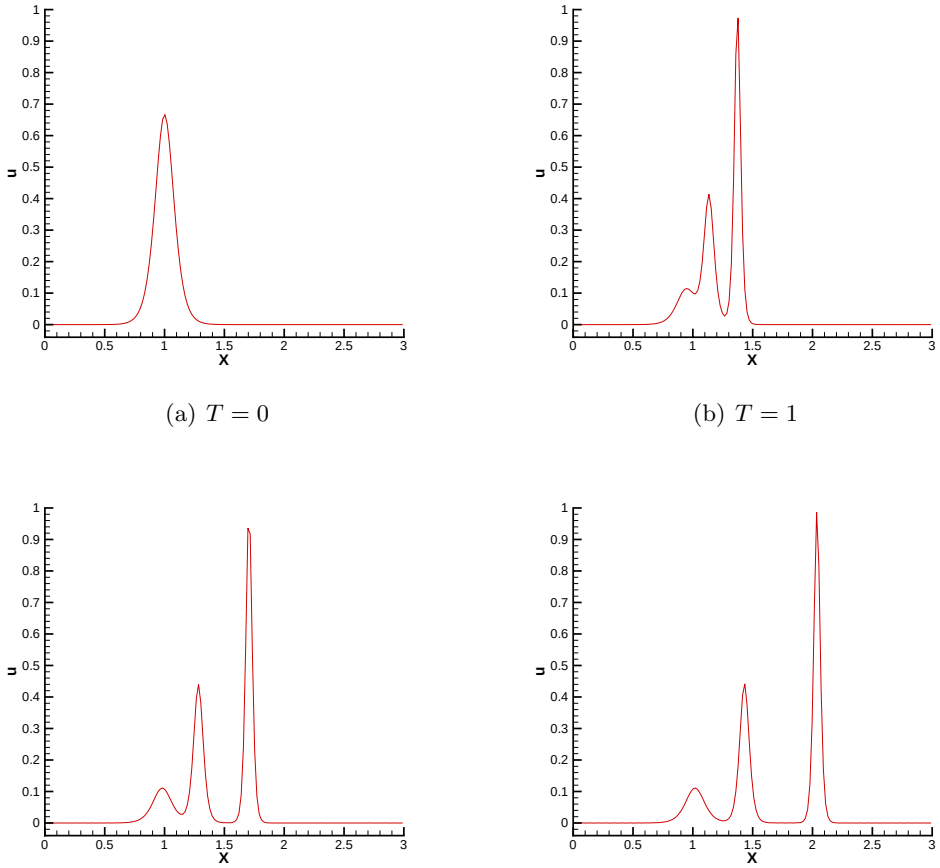

(a) $T = 0$ (b) $T = 1$

(c) $T = 2$ (d) $T = 3$

Figure 3: Example 5.3 (iii): Triple soliton splitting profiles at time $T = 0, 1, 2, 3$.

From these figures we find that all the results are comparable with that showed in [37], where explicit RK methods were used in time discretization. The advantage of adopting IMEX time discretization lies in that larger time step can be taken.

Example 5.4. We test the long time behavior of the schemes for a two-soliton solution of the KdV equation

$$U_t + (U^2/2)_x + U_{xxx} = 0. \tag{5.5}$$

The two-soliton solution is derived from [12] and this example was also tested in [40].

$$U(x,t) = 12\frac{\kappa_1^2 e^{\theta_1} + \kappa_2^2 e^{\theta_2} + 2(\kappa_2 - \kappa_1)^2 e^{\theta_1+\theta_2} + \omega(\kappa_2^2 e^{\theta_1} + \kappa_1^2 e^{\theta_2})e^{\theta_1+\theta_2}}{(1 + e^{\theta_1} + e^{\theta_2} + \omega e^{\theta_1+\theta_2})^2}, \tag{5.6}$$

where $\kappa_1 = 0.4$, $\kappa_2 = 0.6$, $\omega = \left(\frac{\kappa_1-\kappa_2}{\kappa_1+\kappa_2}\right)^2$, $\theta_1 = \kappa_1 x - \kappa_1^3 t + 4$, $\theta_2 = \kappa_2 x - \kappa_2^3 t + 15$. The computational domain is taken as $[-40, 40]$. In this example, we also take $N = 160$ and $\tau = 0.05$. The exact and numerical solutions at time $T = 0, 40, 80, 120$ are displayed in Figure 4, from which we observe that the numerical solutions coincide well with the exact solutions, even at larger computing time.

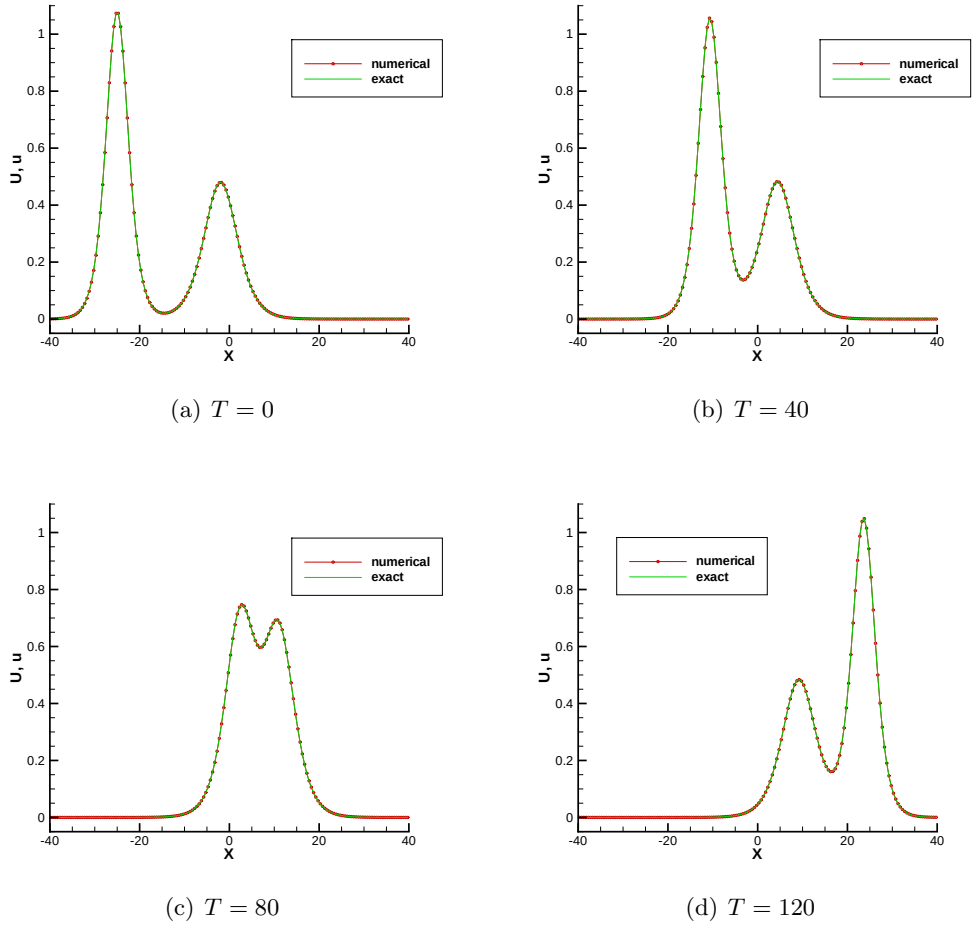

(a) $T = 0$ (b) $T = 40$

(c) $T = 80$ (d) $T = 120$

Figure 4: Example 5.4: two-soliton solutions of KdV equation (5.5) at time $T = 0, 40, 80, 120$.

5.2 Numerical test for the fifth order equation

Example 5.5. In this example, we consider the linear fifth order KdV equation:

$$U_t + cU_x = dU_{xxxxx}, \quad (x,t) \in [0, 2\pi] \times (0, T], \tag{5.7}$$

the initial condition is $U_0(x) = \sin(-x)$ and the exact solution is $U(x,t) = \sin\big((c-d)t - x\big)$. In Table 3, we list the L^2 errors and orders of accuracy of the considered scheme for equation

(5.7) with $d = 1$ and different values $c = 0, 2, 5, 10$. We set the computing time $T = 1$ and the time step $\tau = 0.5h$. We can observe optimal accuracy from the table, also we find that the magnitude error is larger if the coefficient of convection is larger.

Table 3: The L^2 errors and orders of accuracy for equation (5.7) with $d = 1$ and different values of c. $T = 1$, $\tau = 0.5h$.

N	$c = 0$		$c = 2$		$c = 5$		$c = 10$	
	L^2 error	order	L^2 error	order	L^2 error	order	L^2 error	order
40	1.52E-05	–	2.43E-04	–	1.22E-02	–	1.85E-01	–
80	1.91E-06	2.99	3.10E-05	2.97	1.57E-03	2.96	2.60E-02	2.84
160	2.39E-07	3.00	3.93E-06	2.98	1.99E-04	2.98	3.34E-03	2.96
320	2.99E-08	3.00	4.92E-07	3.00	2.49E-05	3.00	4.19E-04	3.00
640	3.73E-09	3.00	6.15E-08	3.00	3.11E-06	3.00	5.25E-05	3.00

Example 5.6. In this example, we consider the Kawahara equation

$$U_t + UU_x + U_{xxx} - U_{xxxxx} = 0, \tag{5.8}$$

with the exact solution presented in [36]

$$U(x,t) = \frac{105}{169}\mathrm{sech}^4\left(\frac{1}{2\sqrt{13}}(x - \frac{36}{169}t)\right). \tag{5.9}$$

The computational domain is $[-40, 40]$, the final computing time is $T = 1$ and $\tau = 0.1h$. We show the results in Table 4, from which we again observe optimal error accuracy.

Table 4: The L^2 errors and orders of accuracy for equation (5.8). $T = 1$, $\tau = 0.1h$.

N	20	40	80	160	320
L^2 error	1.58E-03	1.89E-04	2.43E-05	3.06E-06	3.83E-07
order	-	3.06	2.96	2.99	3.00

Example 5.7. We compute the solitons of the fifth order KdV equations with high nonlinearities [14]

$$U_t + U^pU_x + U_{xxx} - \gamma U_{xxxxx} = 0. \tag{5.10}$$

The following cases were also tested in [29].

(i). $p = 4$, $\gamma > 0$ with the initial condition

$$U(x,0) = \left(\frac{\kappa(p+1)(p+4)(3p+4)}{8(p+2)}\right)^{\frac{1}{p}}\mathrm{sech}^{\frac{4}{p}}\left(\frac{p\sqrt{\kappa(p^2+4p+8)}}{4(p+2)}(x - x_0)\right), \tag{5.11}$$

where $\kappa = \frac{1}{\gamma}\left(\frac{2(p+2)}{p^2+4p+8}\right)^2$. The numerical solution is computed in $[-20, 20]$. We present the numerical results at different time t with different γ and x_0 in Figure 5, which shows that the solutions keep the initial shape and move to the right, and as γ gets smaller the solutions get narrower and higher and move faster.

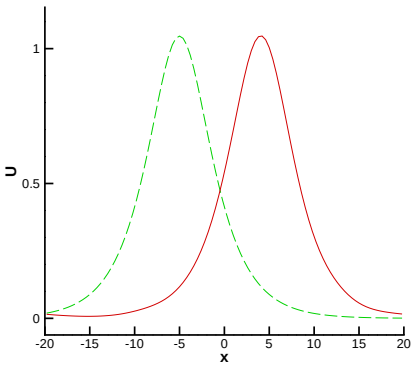

(a) $\gamma = 1$, $x_0 = 5$, $\tau = 0.1$, $N = 100$

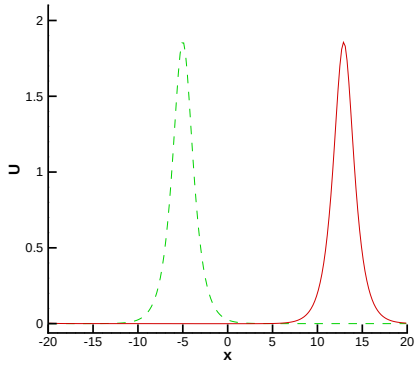

(b) $\gamma = 0.1$, $x_0 = 5$, $\tau = 0.05$, $N = 200$

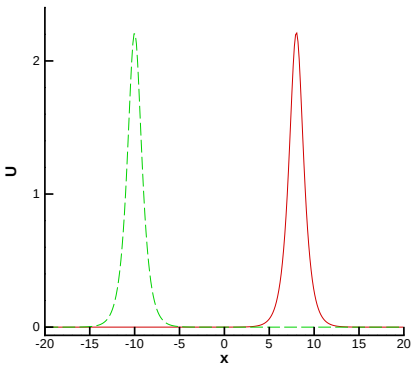

(c) $\gamma = 0.05$, $x_0 = 10$, $\tau = 0.01$, $N = 300$

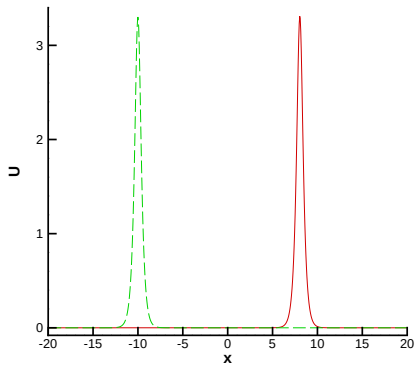

(d) $\gamma = 0.01$, $x_0 = 10$, $\tau = 0.001$, $N = 700$

Figure 5: Example 5.7 (i): Solutions of the nonlinear fifth order KdV equations (5.10) with initial condition (5.11), $p = 4$. Dashed line is the solution at $t = 0$, solid line is the solution at different time t: (a) $t = 100$; (b) $t = 20$; (c) $t = 10$; (d) $t = 2$.

(ii). $p = 2$, $\gamma < 0$ with the initial condition

$$U(x,0) = 3\sqrt{\left|\frac{2}{5\gamma}\right|}\operatorname{sech}\left(\sqrt{\left|\frac{1}{10\gamma}\right|}(x - x_0)\right)\tanh\left(\sqrt{\left|\frac{1}{10\gamma}\right|}(x - x_0)\right), \tag{5.12}$$

where $x_0 = -5$, the numerical solutions with different γ are displayed in Figure 6.

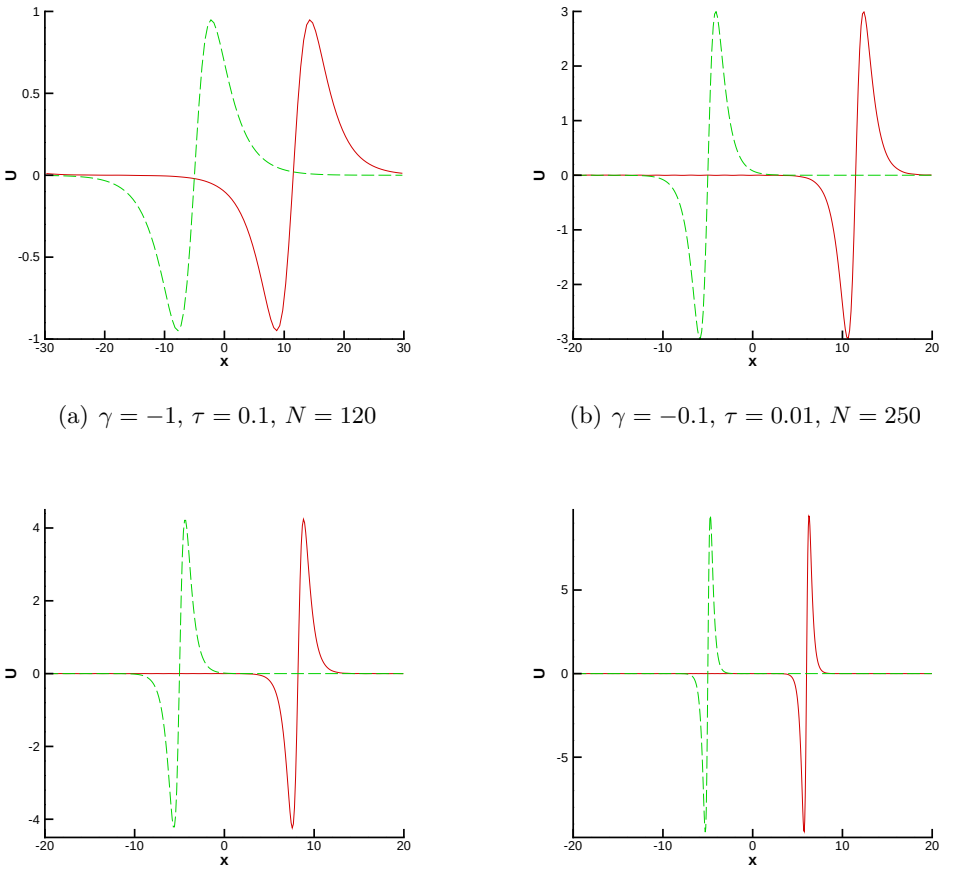

(a) $\gamma = -1$, $\tau = 0.1$, $N = 120$

(b) $\gamma = -0.1$, $\tau = 0.01$, $N = 250$

(c) $\gamma = -0.05$, $\tau = 0.001$, $N = 320$

(d) $\gamma = -0.01$, $\tau = 5 \times 10^{-5}$, $N = 700$

Figure 6: Example 5.7 (ii): Solutions of the nonlinear fifth order KdV equations (5.10) with initial condition (5.12), $p = 2$. Dashed line is the solution at $t = 0$, solid line is the solution at different time t: (a) $t = 150$, $\Omega = [-30, 30]$; (b) $t = 15$, $\Omega = [-20, 20]$; (c) $t = 6$, $\Omega = [-20, 20]$; (d) $t = 1$, $\Omega = [-20, 20]$.

Here we repeat the examples considered in [29] and comparable results are obtained. However, we can take lager time step and only need to solve a linear system. Thus, the proposed scheme is more efficient especially for nonlinear equations with higher order dispersion terms ($\gamma \neq 0$).

Example 5.8. In this example, we show the soliton interaction for the Kawahara equation [3, 29]:

$$U_t + 2UU_x + U_{xxx} - 0.1U_{xxxxx} = 0. \tag{5.13}$$

(i). The double soliton collision case with the initial condition

$$U(x,0) = \frac{105}{338\alpha_1}\text{sech}^4\left(\frac{1}{2\sqrt{13\alpha_1}}(x-x_1)\right) + \frac{105}{338\alpha_2}\text{sech}^4\left(\frac{1}{2\sqrt{13\alpha_2}}(x-x_2)\right), \tag{5.14}$$

where $\alpha_1 = \frac{0.04\times 338}{105}$, $\alpha_2 = \frac{0.15\times 338}{105}$, $x_1 = -8$, $x_2 = -2$. The numerical solution is computed in $[-18, 18]$. We present the numerical solutions with different time T in Figure 7.

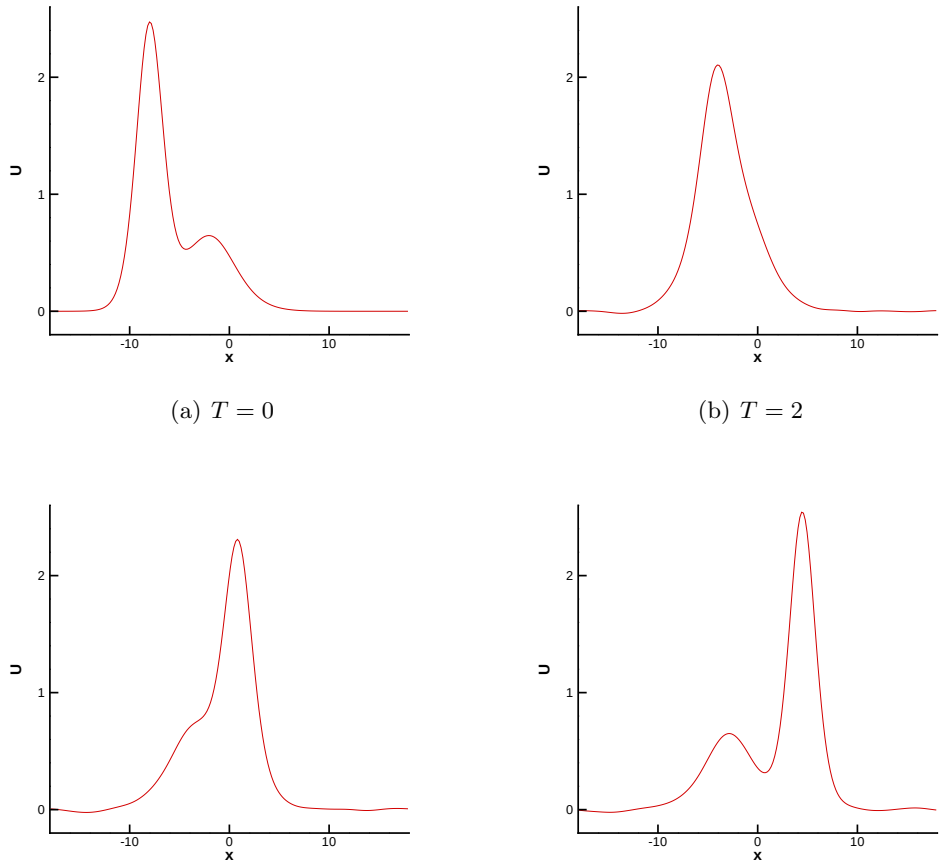

(a) $T = 0$ (b) $T = 2$

(c) $T = 4$ (d) $T = 6$

Figure 7: Example 5.8 (i): Solutions of the Kawahara equations (5.13) with initial condition (5.14) at different time, $\tau = 0.1$, $N = 200$.

(ii). The interaction of three solitary waves with the initial condition

$$U(x,0) = \sum_{s=1}^{3} \frac{1}{\alpha_s} \mathrm{sech}^4 \left(\frac{1}{2\sqrt{13\alpha_s}} (x - x_s) \right), \tag{5.15}$$

where $\alpha_1 = 0.25$, $\alpha_2 = 0.35$, $\alpha_3 = 0.45$, $x_1 = -11$, $x_2 = -9$, $x_3 = -7$. The numerical solution is computed in $[-20, 20]$. The numerical solutions with different time T are presented in Figure 8.

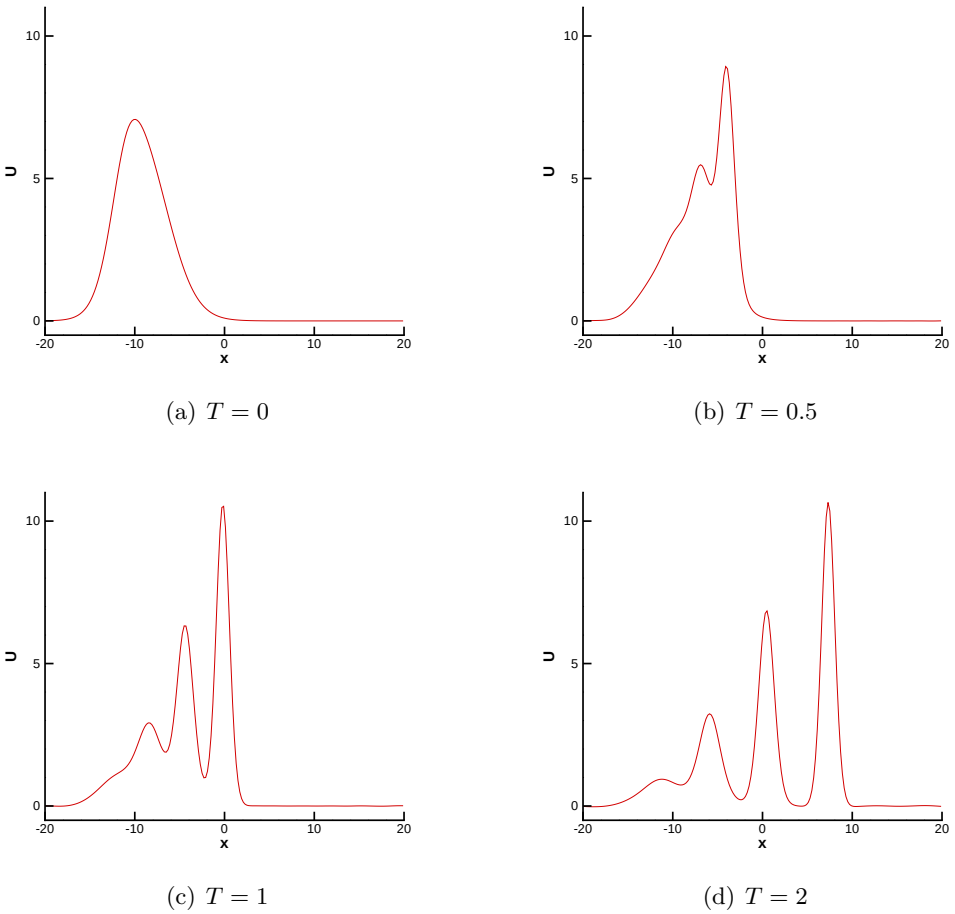

(a) $T = 0$ (b) $T = 0.5$

(c) $T = 1$ (d) $T = 2$

Figure 8: Example 5.8 (ii): Solutions of the Kawahara equations (5.13) with initial condition (5.15) at different time, $\tau = 0.01$, $N = 200$.

From these figures we find that all the results are comparable with that showed in [29].

6 Conclusion

The unconditional stability and optimal error estimates of a third order IMEX-RK time discretization method coupled with LDG spatial discretization are studied for the third

order and the fifth order wave equations (1.1) and (1.2) without the convection term. With the help of the temporal difference technique, we establish the desired energy equations by finding out the stability from the temporal differences and by constructing a semi-negative definite symmetric form related to the spatial discretization for the third/fifth order derivative terms. In addition, we also obtain optimal error estimates for the considered schemes by adopting a proper projection. The proof line given in this paper might help us to investigate the stability and error estimates of IMEX-LDG schemes for high order wave equations containing lower order spatial derivative terms, which will constitute our future work.

References

[1] U. Ascher, S. Ruuth, and R. Spiteri, *Implicit-explicit Runge-Kutta methods for time-dependent partial differential equations*, Appl. Numer. Math., 25 (1997), pp. 151–167.

[2] U. Ascher, S. Ruuth, and B. Wetton, *Implicit explicit methods for time-dependent partial-differential equations*, SIAM J. Numer. Anal., 32 (1995), pp. 797–823.

[3] A. Bashan, *An efficient approximation to numerical solutions for the Kawahara equation via modified cubic B-spline differential quadrature method*, Mediterranean Journal of Mathematics, 16 (2019).

[4] T. B. Benjamin, J. L. Bona, and J. J. Mahony, *Model equations for long waves in nonlinear dispersive systems*, Phil. Trans. Roy. Soc. London Ser. A, 272 (1972), pp. 47–78.

[5] H. Bi and M. Zhang, *Stability analysis and error estimates of implicit Runge-Kutta local discontinuous Galerkin methods for linear bi-harmonic equation*, Comput. Math. Appl., 149 (2023), pp. 211–220.

[6] S. Boscarino, L. Pareschi, and G. Russo, *Implicit-explicit Runge-Kutta schemes for hyperbolic systems and kinetic equations in the diffusion limit*, SIAM J. Sci. Comput., 35 (2011), pp. A22–A51.

[7] M. Calvo, J. de Frutos, and J. Novo, *Linearly implicit Runge-Kutta methods for advection-reaction-diffusion equations*, Appl. Numer. Math., 37 (2001), pp. 535–549.

[8] P. Castillo, B. Cockburn, D. Schotzau, and C. Schwab, *Optimal a priori error estimates for the hp-version of the local discontinuous Galerkin method for convection-diffusion problems*, Math. Comput., 71 (2002), pp. 455–478.

[9] B. Cockburn and C.-W. Shu, *The local discontinuous Galerkin method for time-dependent convection-diffusion systems*, SIAM J. Numer. Anal., 35 (1998), pp. 2440–2463.

[10] G. J. Cooper and A. Sayfy, *Additive Runge-Kutta methods for stiff ordinary differential equations*, Math. Comput., 40 (1983), pp. 207–218.

[11] S. Cox and P. Matthews, *Exponential time differencing for stiff systems*, J. Comput. Phys., 176 (2002), pp. 430–455.

[12] Y. Cui and D. K. Mao, *Numerical method satisfying the first two conservation laws for the Korteweg-de Vries equation*, J. Comput. Phys., 227 (2007), pp. 376–399.

[13] A. Debussche and J. Printems, *Numerical simulation of the stochastic Korteweg-de Vries equation*, Phys. D, 134 (1999), pp. 200–226.

[14] B. Dey, A. Khare, and C. N. Kumar, *Stationary solitons of the fifth order KdV-type equations and their stabilization*, Physics Letters A, 223 (1996), pp. 449–452.

[15] B. Dong and C.-W. Shu, *Analysis of a local discontinuous Galerkin method for linear time-dependent fourth-order problems*, SIAM J. Numer. Anal., 47 (2009), pp. 3240–3268.

[16] A. Dutt, L. Greengard, and V. Rokhlin, *Spectral deferred correction methods for ordinary differential equations*, BIT, 40 (2000), pp. 241–266.

[17] D. Dutykh, T. Katsaounis, and D. Mitsotakis, *Finite volume methods for unidirectional dispersive wave models*, Int. J. Numer. Methods Fluids, 71 (2013), pp. 717–736.

[18] C. Kennedy and M. Carpenter, *Additive Runge-Kutta schemes for convection-diffusion-reaction equations*, Appl. Numer. Math., 44 (2003), pp. 139–181.

[19] D. Levy, C.-W. Shu, and J. Yan, *Local discontinuous Galerkin methods for nonlinear dispersive equations*, J. Comput. Phys., 196 (2004), pp. 751–772.

[20] Y. Li, C.-W. Shu, and S. Tang, *An ultra-weak discontinuous Galerkin method with implicit-explicit time-marching for generalized stochastic KdV equations*, J. Sci. Comput., 82 (2020).

[21] A. Marchenko, *Long waves in shallow liquid under ice cover*, J. Appl. Math. Mech., 52 (1988), pp. 180–183.

[22] Z. Sun, Y. Wei, and K. Wu, *On energy laws and stability of Runge-Kutta methods for linear seminegative problems*, SIAM J. Numer. Anal., 60 (2022), pp. 2448–2481.

[23] M. Tan, J. Cheng, and C.-W. Shu, *Stability of high order finite difference and local discontinuous Galerkin schemes with explicit-implicit-null time-marching for high order dissipative and dispersive equations*, J. Comput. Phys., 464 (2022).

[24] H. Wang, F. Li, C.-W. Shu, and Q. Zhang, *Uniform stability for local discontinuous Galerkin methodswith implicit-explicit Runge-Kutta time discretizations for linear convection-diffusion equation*, Math. Comput., 92 (2023), pp. 2475–2513.

[25] H. Wang, C.-W. Shu, and Q. Zhang, *Stability and error estimates of local discontinuous Galerkin methods with implicit-explicit time-marching for advection-diffusion problems*, SIAM J. Numer. Anal., 53 (2015), pp. 206–227.

[26] H. Wang, Q. Tao, C.-W. Shu, and Q. Zhang, *Analysis of local discontinuous Galerkin methods with implicit-explicit time marching for linearized KdV equations*, SIAM J. Numer. Anal., (accepted).

[27] H. Wang, Q. Zhang, and C.-W. Shu, *Stability analysis and error estimates of local discontinuous Galerkin methods with implicit-explicit time-marching for the time-dependent fourth order PDEs*, ESAIM: M2AN, 51 (2017), pp. 1931–1955.

[28] Y. Xia, Y. Xu, and C.-W. Shu, *Efficient time discretization for local discontinuous Galerkin methods*, Discrete Cont Dyn-B, 8 (2007), pp. 677–693.

[29] Y. Xu and C.-W. Shu, *Local discontinuous Galerkin methods for three classes of nonlinear wave equations*, J. Comput. Math., 22 (2004), pp. 250–274.

[30] ——, *Local discontinuous Galerkin methods for nonlinear Schrödinger equations*, J. Comput. Phys., 205 (2005), pp. 72–97.

[31] ——, *Local discontinuous Galerkin methods for the Kuramoto-Sivashinsky equations and the Ito-type coupled KdV equations*, Comput. Methods Appl. Mech. Eng., 195 (2006), pp. 3430–3447.

[32] ——, *A local discontinuous Galerkin method for the Camassa-Holm equation*, SIAM J. Numer. Anal., 46 (2008), pp. 1998–2021.

[33] ——, *Local discontinuous Galerkin methods for high-order time-dependent partial differential equations*, Comm. Comput. Phys., 7 (2010), pp. 1–46.

[34] ——, *Local discontinuous Galerkin methods for the Degasperis-Procesi equation*, Comm. Comput. Phys., 10 (2011), pp. 474–508.

[35] Y. Xu, Q. Zhang, C.-W. Shu, and H. Wang, *The L^2-norm stability analysis of Runge-Kutta discontinuous Galerkin methods for linear hyperbolic equations*, SIAM J. Numer. Anal., 57 (2019), pp. 1574–1601.

[36] Y. Yamamoto and E. Takizawa, *On a solution of nonlinear time-evolution equation of fifth order*, J. Phys. Soc. Japan, 50 (1981), pp. 1421–1422.

[37] J. Yan and C.-W. Shu, *A local discontinuous Galerkin method for KdV type equations*, SIAM J. Numer. Anal., 40 (2002), pp. 769–791.

[38] C. Zhang, Y. Xu, and Y. Xia, *Local discontinuous Galerkin methods to a dispersive system of KdV-type equations*, J. Sci. Comput., 86 (2021).

[39] Q. Zhang and F. Gao, *A fully-discrete local discontinuous Galerkin method for convection-dominated Sobolev equation*, J. Sci. Comput., 51 (2012), pp. 107–134.

[40] Q. Zhang and Y. Xia, *Conservative and dissipative local discontinuous Galerkin methods for Korteweg-de Vries type equations*, Comm. Comput. Phys., 25 (2019), pp. 532–563.